SAND2015-10399J

Deflagration-to-Detonation Transition in High Pressure Ethylene/Nitrous Oxide Mixtures in Small and Large L/d Tubes

Prashanth Bangalore Venkatesh[1], Scott E. Meyer[2], Sally P.M. Bane[3]
School of Aeronautics & Astronuatics
Purdue University, 701 W. Stadium Ave., West Lafayette, IN 47906

Mark C. Grubelich[4]
Sandia National Laboratories
PO Box 5800, Mail Stop 1033, Albuquerque, NM 87185, USA

Abstract

Nitrous oxide has been a compound of interest for nearly a century due to its exothermic decomposition and oxygen production. Also, concerns about the safety of nitrous oxide have arisen in the nuclear industry, as it has been observed that stored nuclear waste generates and retains large amounts of flammable gases such as hydrogen and ammonia along with nitrous oxide. These gases result in flammable concentrations in tanks when they are released. Nitrous oxide has also been investigated as a rocket propellant for both hybrid and bipropellant rockets. Therefore, understanding the combustion characteristics, particularly under high pressure, of mixtures of fuel with nitrous oxide is highly important. The present work investigates the high pressure combustion characteristics of a stoichiometric mixture of ethylene and nitrous oxide ($C_2H_4 + 6N_2O$) in an alloy steel vessel with a 4 in. inner diameter and an internal length of 24.5 in. The combustion is initiated by energizing either a nichrome wire or an electric match connected to leads in the vessel. The experimental setup accommodates four high pressure

---

[1] Ph.D. Student: pbangalo@purdue.edu
[2] Managing Director for Maurice J. Zucrow Laboratories: meyerse@purdue.edu
[3] Assistant Professor: sbane@purdue.edu
[4] Distinguished Member of the Technical Staff: mcgrube@sandia.gov

(100,000 psia) transducers to measure pressure peaks at positions along the length of the vessel during the propagation of the combustion wave. Based on the time at which these peak pressures are recorded by the transducers it is possible to estimate the propagation speed of the combustion wave. The focus of this series of experiments is to investigate the dependence of combustion pressures, propagation speeds, and deflagration-to-detonation transition (DDT) on initial pressures of a stoichiometric mixture of ethylene and nitrous oxide. Experiments were carried out at initial pressures of 100 psia, 125 psia, 150 psia, 200 psia, 337 psia, and 500 psia. Overdriven detonations of different strengths were observed during each of the tests. The transducers recorded elevated pressures that were significantly higher than the CJ values. The surprising experimental results are discussed and explained using theoretical considerations of flame acceleration, detonation, and DDT mechanisms. These experiments were conducted at Zucrow Laboratories, Purdue University.

Keywords: Detonations, DDT, High pressures, Ethylene, Nitrous-oxide

1. Introduction

The decomposition and combustion properties of nitrous oxide (N_2O) have been studied for nearly a century. Technical interest in nitrous oxide intensified in the 1960s[5] because of the compounds positive heat of formation, and so heat is released during decomposition. Also, upon complete dissociation the products are pure nitrogen (N_2) and oxygen (O_2). These characteristics made nitrous oxide a unique oxidizer for combustion systems, and ignited interest in using nitrous oxide in supersonic wind tunnels to increase the enthalpy. A great deal of work was done by the Air Force in the 1960s to characterize the decomposition and combustion of nitrous oxide. Laughrey et al. [3] studied the decomposition and detonability of pure nitrous oxide at elevated temperatures and pressures, and while they were not

---

[5] Prior to the 1960s the Germans tested a nitrous oxide and coal hybrid rocket at I.G. Farben. The rocket, developed by L. Andrussow, O. Lutz and W. Noeggerath, produced 10-kN thrust for 120s [1]. This was followed by the usage of nitrous oxide in aircraft engines that was used by the Luftwaffe in World War II to improve high-altitude performance. The gas was liquefied and sprayed into the intakes using the injecting system Gring Mischung 1 or GM-1. Around the same time NACA investigated supercharging radial engines with nitrous oxide [2].

able to achieve detonation they did observe high rates of chemical reaction they categorized as explosions. They concluded that it appears quite possible that a detonation wave in nitrous oxide can be established in a longer tube. In the next year, Jost et al. [4] studied the detonation and chemical kinetics of hydrazine and nitrous oxide to assess the viability of nitrous oxide as an oxidizer for rocket propulsion. They measured detonation speeds of hydrazine-nitrous oxide mixtures at very low initial pressures (on the order of 0.1 atm) and found the speed to be close to the ideal Chapman-Jouguet (CJ) detonation velocity. At the same time, Bollinger et al. [5] studied the detonation velocities and induction distances in hydrogen-nitrous oxide mixtures at initial pressures of 1, 5, and 10 atm. They ignited the mixtures in a tube with a 79 mm inner diameter via a copper wire, and then measured the speed of the propagating flame until it accelerated to the CJ detonation velocity. They found that the induction distance decreased with increasing initial pressure, and that at 10 atm the induction distance could be as small as 0.3 m.

In the last few decades, research on nitrous oxide has focused on the explosion hazard posed by fuel-nitrous oxide mixtures, as nitrous oxide is used in a variety of industrial and aerospace applications. One particular area of concern is the handling and storage of nuclear waste, as it is known that the waste can generate and retain various amounts of flammable gases and nitrous oxide. These gases are released after sufficient build-up and result in combustible mixtures in the tanks [6]. To address this issue, Kaneshige and colleagues at the California Institute of Technology performed experimental studies of detonations in mixtures of fuels with N_2O, O_2, and N_2; they first studied detonations in hydrogen (H_2) and methane (CH_4) [7] and then ammonia (NH_3) [8]. The detonations were produced using direct initiation in a large (280 mm inner diameter, 7.5 m in length) detonation tube, and the detonation velocity and cell size were measured and compared with calculated theoretical values. Mével et al. [9] and Bane et al. [10] have recently studied the combustion characteristics of hydrogen-nitrous oxide mixtures at low pressures, measuring the laminar burning speeds and comparing with chemical kinetics calculations. Recent accidents involving stored nitrous oxide have led to concern over its explosion hazard, either from exothermic decomposition or through fuel contamination of stored nitrous oxide creating an explosive mixture [11].

Finally, additional interest in nitrous oxide has arisen in the past several years as it is being more widely considered as a “safe,” clean oxidizer for rocket propulsion systems, because it is suitable as both a monopropellant or as a bipropellant [11]. Grubelich et al. [12] replaced toxic or cryogenic oxidizers typically used in hybrid engines with nitrous oxide and tested it with hydroxyl terminated polybutadiene (HTPB) as the fuel. According to their work, the nitrous oxide hybrid engine can have longer burn times than conventional solid propellant rocket motors for a given geometry. Later, Tyll et al. [13] tested nitrous oxide with propane in a bipropellant rocket engine. The nitrous oxide was catalytically decomposed and the exothermic nature of this process ignited the propane to produce sustained combustion. Both these propellants can be stored as high-pressure liquids which facilitate self-pressurization. Tyll and co-workers proposed that performance improvements could be achieved by replacing the low vapor pressure propane with ethylene, which has a similar vapor pressure as nitrous oxide. Using ethylene as the fuel, their analysis predicted an increase of the specific impulse by several seconds. In addition, DiSalvo et al. [14] tested their patented constant volume rocket motor with nitrous oxide and propane in pulsed motor mode generating brief chamber pressure pulses on the order of 500-700 psia using injector inlet pressures of only 40-50 psia. In 2011, DARPA announced the Airborne Launch Assist Space Access (ALASA) program designed to produce a rocket capable of launching a 100 lb satellite into low Earth orbit with Boeing contracted to develop the launch system. Boeing intends to lower the complexity of the launch vehicle and thus costs by powering the rocket with a monopropellant comprised of a combination of nitrous oxide and acetylene, mixed in the same tank and stored at a temperature slightly below room temperature. Along with simplicity this combination is expected to produce a specific impulse close to a LOX - RP1 combination [15].

In the present work, the combustion of nitrous oxide with a simple hydrocarbon, ethylene, at high initial pressures is investigated. According to Joannon [16], one of the critical parameters that determines the detonability of given gas mixture is the initial pressure, and so the primary focus of the current work was to investigate the effect of initial pressure on DDT. A series of experiments were conducted using a stoichiometric ethylene-nitrous oxide mixture in a round, smooth-walled tube with initial pressures of 125 to 337 psi. A low-energy ignition mechanism (heated wire) was used to prevent direct initiation of a detonation via shock, and the flame acceleration and subsequent deflagration-to-detonation transition (DDT) was observed.

2. Methods

The experiments were performed at the High Pressure Lab at Purdues Zucrow Laboratories in an “R” series reactor vessel with an inner diameter of 4.0 in., designated the R4 reactor vessel. The vessel was designed and manufactured by High Pressure Equipment Company. The reactor has an internal length of 24.5 in., wall thickness of 2.0 in and is constructed of alloy steel (4340). The reactor vessel was designed for a static pressure of 20,000 psia and hydrostatically tested to 30,000 psia. As shown in Figure 1 and Figure 2, the vessel has three ports on the side wall and one port through the cover (labeled 1 in Figure 1) with four PCB 109C11 pressure transducers. The installed transducers are connected to a high frequency data acquisition system via signal conditioning and record explosion pressures at these points in the vessel. Data is recorded at 600,000 samples/s/channel. The setup is equipped with plumbing to supply nitrogen from the high pressure supply and ethylene and nitrous oxide from respective bottles. The high pressure nitrogen is used to pressure leak test and purge the vessel before and after every test. The plumbing for the fuel and oxidizer includes separate sonic venturis and low frequency pressure transducers that are used to set mass flow rates of the two gases resulting in the appropriate final pressure for each test. Separate check valves are connected at the inlet of the vessel to prevent back flow of initial gas mixture and combustion gases into the supply cylinders. The partial pressures of ethylene and nitrous oxide supplied to the vessel are calculated to achieve a stoichiometric fuel-oxidizer mixture. The reactor is heated to approximately 100°F using tape heaters to prevent condensation at high pressures.

Ignition of the mixture is achieved using a heated nichrome wire mounted on the end wall of the reactor and the wire was energized using an 18 V Li-Po battery through a solid state relay. After setting up the nichrome wire and pressure leak checking before each test firing, the vessel is purged with nitrogen and then with nitrous oxide before pressurization with ethylene and nitrous oxide to the calculated pressures. Purging with nitrous oxide prior to charging the vessel ensured an atmosphere of nitrous oxide at ambient pressure thereby minimizing the presence of any other gases in the vessel. Pressurizing the vessel with ethylene and nitrous oxide is controlled by auto-sequence via a LabVIEW interface, and the gases are allowed approximately 60 seconds to mix before igniting the mixture. As part of the auto-sequence, the interface recorded data from the low frequency instrumentation on the setup at a sampling rate of 100 samples/s/channel. This data was used to estimate the actual O/F, initial pressure and temperature of the gas mixture.

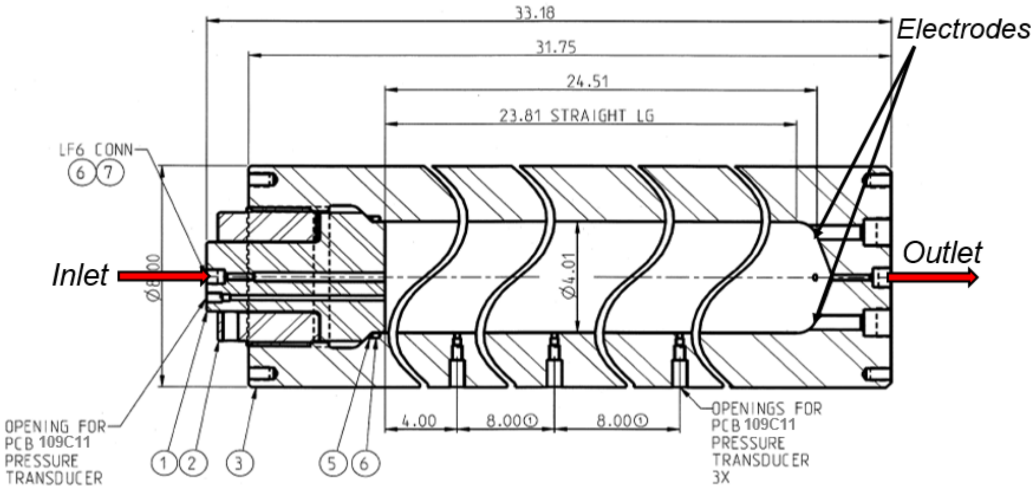

Figure 1: Diagram of the high-pressure reactor.

After each test the combustion gases are expelled through a vent line. The vent line consists of a safety head which houses a rupture disc rated at 20,000 psi, a pneumatically actuated high pressure 2-way ball valve, a low frequency pressure transducer and a low pressure pneumatic ball valve, in that order. The high pressure valve is closed prior to ignition of the gas mixture to contain the combustion gases in the vessel. This valve is left open when charging the vessel and the low pressure valve is closed and the initial pressure in the vessel is measured using the low frequency pressure transducer.

For comparison with the experimental results, the CJ detonation velocities and CJ pressures for a stoichiometric ethylene-nitrous oxide mixture at the elevated initial pressures were calculated. The calculations were performed using the Shock and Detonation Toolbox developed by Browne et al. [17]. The toolbox is implemented in Cantera, a suite of object-oriented software tools for problems involving chemical kinetics, thermodynamics and transport processes [18]. The results of these calculations are presented in Section 3.2.

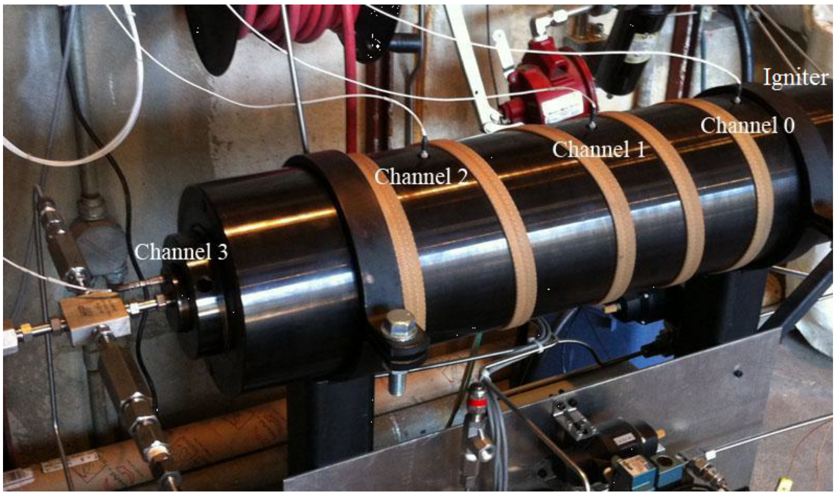

Figure 2: Photograph of the reactor vessel with the locations of the pressure transducers and igniter indicated.

3. Results and Discussion

3.1. Experimental Results

Experimental runs with initial pressures of 125 psia, 150 psia, 200 psia, 337 psia and 500 psia were conducted and the explosion pressures for each run are given in Table 1. Based on the time instances of these pressure peaks and using the distance between pressure transducers (PTs), the propagation speeds of the combustion waves were estimated and are presented in Table 2. The CJ detonation velocities, D_{CJ}, calculated using Cantera for each case, are also given in Table 2. The pressure data logged from the transducers during each test were plotted versus time. Example plots from a 150 psia test and a 200 psia test are shown in Figures 3 and 4. Note that in the plot for the test with initial pressure 337 psia, the pressure plot for the third transducer on the side wall failed to provide useful data and hence was not included in the tables. The measured pressures and estimated velocities from these tests are plotted versus transducer locations and shown in Figures 5 and 6, respectively. The sudden rise in the pressure peak observed in Figure 5 indicates that the combustion wave has already transitioned to a detonation at this location. This behavior is observed at location 1 during all the tests presented.

Table 1: Combustion peak pressures as detected by the transducers.

Test No.	**Initial Conditions**			**CJ Pressure [psia]**	**Peak Pressures [psia]**			
	O/F	ϕ	**Pressure [psia]**		$\mathbf{P}_0$	$\mathbf{P}_1$	$\mathbf{P}_2$	$\mathbf{P}_3$
30	9.61	0.98	125	4919	12600	12669	16671	41316
31	9.13 [6]	1.03	150	5933	13610	17888	14295	27628
32	9.13 [6]	1.03	200	7974	24512	15406	29192	36350
33	8.87	1.06	200	7974	12474	12222	13508	31326
34	9.38	1.00	337	13195	36668	25338	-	61369

Table 2: Detonation velocities and overdriven factors.

Test No.	**Initial Conditions**			**Calculated CJ Velocity $\mathbf{D}_{\mathbf{CJ}}$ [m/s]**	**Velocities [m/s] & Overdriven Factors ($\mathbf{D}/\mathbf{D}_{\mathbf{CJ}}$)**			
	O/F	ϕ	**Pressure [psia]**		$\mathbf{D}_0$	$\mathbf{D}_1$	$\mathbf{D}_2$	$\mathbf{D}_3$
30	9.61	0.98	125	2279	85	2677	2736	1807
					0.04	**1.17**	**1.20**	**0.79**
31	9.13 [6]	1.03	150	2285	62	3328	2414	2090
					0.03	**1.46**	**1.06**	**0.91**
32	9.13 [6]	1.03	200	2295	74	3003	2798	1911
					0.03	**1.31**	**1.22**	**0.83**
33	8.87	1.06	200	2295	68	2239	2323	1807
					0.03	**0.98**	**1.01**	**0.79**
34	9.38	1.00	337	2309	85	2863	-	2293
					0.04	**1.24**	**-**	**0.99**

The most striking result is the very high pressures recorded during the experiment. For the experiment with the lowest initial pressure of 125 psi, the predicted CJ detonation pressure is approximately 5000 psi. However, the first transducer (P_0) measures a pressure more than twice the CJ value, 12,600 psi. Similar results are also observed for the tests at higher initial pressures, with the measured peak pressure at the first transducer exceeding the predicted CJ value by a factor of 2 to 3. However, the average velocity

---

[6] Approximate O/F value due to loss of zero data.

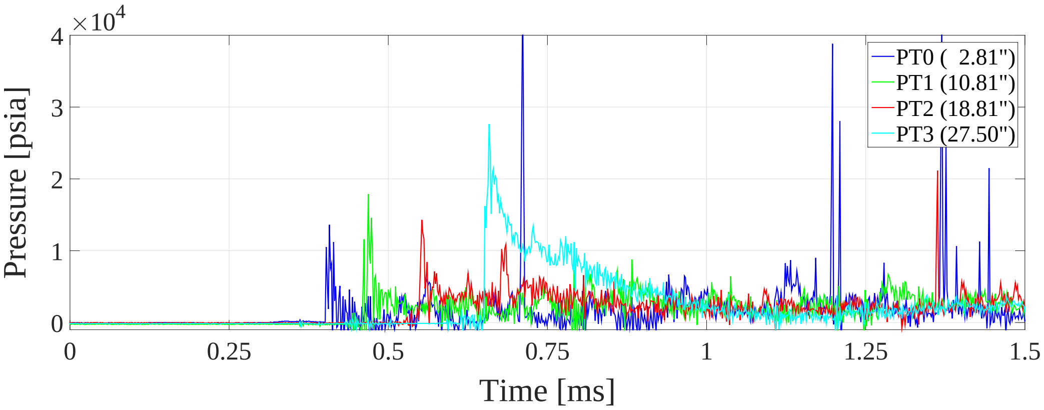

Figure 3: Pressure plots for 150 psia stoichiometric ethylene and nitrous oxide (Test 31).

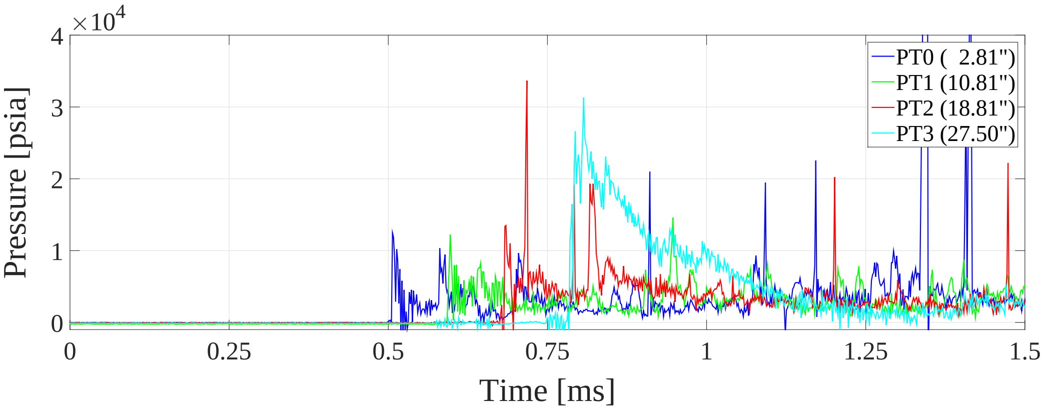

Figure 4: Pressure plots for the second 200 psia stoichiometric ethylene and nitrous oxide (Test 33).

of the combustion wave between the igniter and the first transducer was on the order of 90 m/s, well below the CJ detonation velocity. The heated nichrome wire ignites the gas thermally and does not produce a shock, which is necessary to directly initiate a detonation. Since the energy of the igniter is far too low to directly initiate a detonation, it must first initiate a deflagration that then transitions to a detonation between the ignition point and the first transducer.

Lee [19] discusses in-depth the mechanisms for deflagration-to-detonation transition (DDT) based on investigations of detonations in smooth tubes. In the current experiments, the mechanism is believed to be rapid acceleration

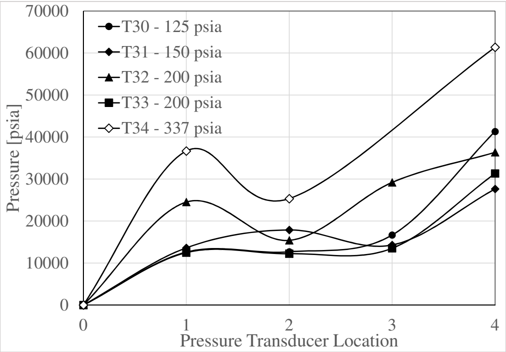

Figure 5: Pressure peaks vs. transducer locations for all tests.

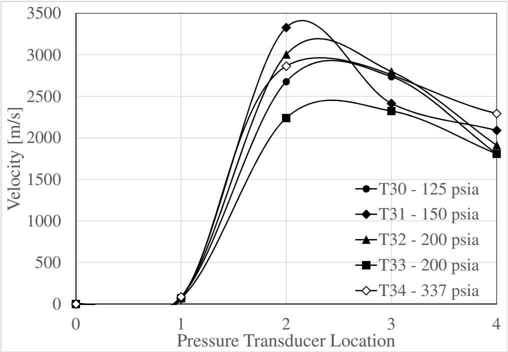

Figure 6: Velocity vs. transducer locations for all tests.

of the deflagration immediately following ignition. Mixtures of fuels with nitrous-oxide can produce highly unstable and turbulent deflagrations that rapidly self-accelerate. For example, Bane et al. [10] noted that undiluted hydrogen-nitrous oxide flames became unstable nearly immediately following ignition, even at low pressures. The flame was observed to be highly turbulent, with wrinkles in the flame surface creating an elaborate cellular structure. This increase in the flame surface area causes a dramatic increase in the burning rate and hence the flame accelerates significantly.

Similarly, the ethylene-nitrous oxide mixture at elevated pressures would likely also be highly unstable and become a turbulent flame immediately following ignition. The turbulent flame produces pressure waves upstream that pre-pressurize the unburned gas. These waves reflect off the reactor walls and further interact with the flame front, magnifying the flame front turbulence and enhancing the flame acceleration. As explained by Lee [19], if the flame acceleration mechanisms can bring the flame to a critical deflagration speed (usually on the order of half the CJ speed), the flame velocity will then accelerate rapidly and the flame will undergo transition to detonation. Depending on the size of the initial flame velocity, DDT can spontaneously occur within a couple of tube diameters [19]. The first transducer on the reactor vessel is loaded at a distance of 2.81 in. from the nichrome wire. During each test the flame transitioned to a detonation within this distance which is approximately 0.7 tube diameters. This is an extremely short distance for DDT to occur, so the combined effects of the inherent instability of the mixture, the high initial pressure, and the flame confinement must promote extremely rapid flame acceleration.

After the first transducer, the pressure changes moderately at the second (P_1) and third (P_2) transducers, but the average combustion wave speed is significantly higher, and in most cases larger than the CJ velocity. This suggests that the detonation is overdriven, with the overdrive factor (ratio of the velocity to the CJ velocity) also given in Table 2. Generally, an overdriven detonation is obtained from using extremely large ignition energy, i.e. an exploding wire that generates a strong shock wave. In this case, however, the ignition energy is far too small. A possible mechanism, as discussed by Lee [19], is the generation of a shock wave by localized explosions. As the propagating deflagration front interacts with the reflected pressure waves in the vessel, the gas near the front is continuously compressed and heated, which can result in a localized explosion directly in front of the flame. This explosion creates a shock wave that will have a velocity significantly higher than a CJ detonation; as the detonation forms from the shock wave, it will initially be overdriven. Therefore, we postulate that in these experiments there occur one or more localized explosions near the deflagration front that result in an overdriven detonation wave. This would also explain the extremely high pressures, as even a small overdrive factor results in a dramatic increase in the detonation pressure. Detonations are also very unstable, and this is further demonstrated by the significant variation in the pressures from one transducer to the next, as in the 337 psia initial pressure test, and between tests at the same initial pressure, as with the two tests at 200 psia. Such large variation in the pressure is not unexpected, and the transition from deflagration to detonation is a complex phenomenon with a certain amount of variation observed in the location of transition.

Finally, the fourth pressure transducer (P_3) measures the reflected detonation pressure at the end of the tube. If the detonation reaching the end wall is in fact still overdriven, then the reflected pressures measured by the transducer are consistent with what the theory predicts. From the experiments conducted thus far, it appears that the high initial pressure, sensitivity of the flammable mixture, and the high level of confinement in the tube result in nearly immediate DDT and a highly unstable, overdriven detonation reflecting from the end wall. According to Lee [19], the overdriven detonation would decay in time to either a stable CJ detonation or an unstable detonation with a velocity oscillating around the CJ velocity. However, in these experiments the overdriven detonation does not propagate a sufficient distance to decay to a near-CJ detonation.

3.2. Comparison with Theoretical Predictions

The theoretical detonation pressures and temperatures for a range of initial pressures of the gas mixture in the vessel were calculated using Cantera to compare with the experimental pressure measurements. These calculations were performed for the following fuel-oxidizer combinations: ethylene-nitrous oxide (combination used in the experiments), ethylene-air, and ethylene-oxygen. The combustion calculations with air and oxygen are presented here for comparison and to understand the effect of different oxidizers. The results of the calculations are shown in Figures 7 and 8.

The calculations were carried out at an initial temperature of 80.3 ^{o}F (300 K). For all cases, the CJ detonation pressure increases linearly with increasing initial pressure in the vessel. The theoretical CJ detonation pressures are highest with nitrous oxide as the oxidizer and lowest with air as the oxidizer; the increase in the combustion pressure when changing from oxygen to nitrous oxide is relatively small, approximately 11-13%. The theoretical combustion temperatures with oxygen as the oxidizer are higher than those calculated with nitrous oxide and air as oxidizers. As discussed previously, the CJ detonation pressures are significantly lower than the pressures observed in the experiment. This discrepancy occurs because the detonation achieved in the vessel is not a CJ detonation but rather an unstable, overdriven detonation.

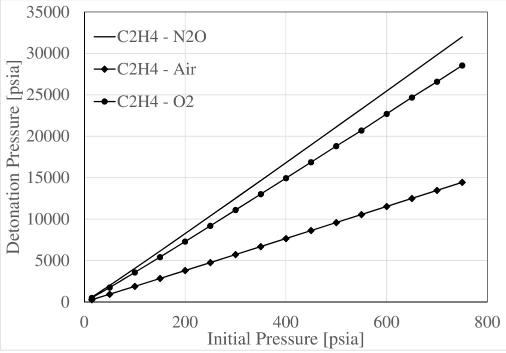

Figure 7: Theoretical CJ detonation pressures for stoichiometric gas mixtures vs. initial pressure.

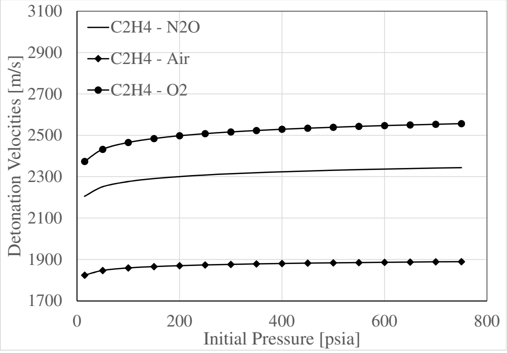

Figure 8: Theoretical CJ detonation velocities for stoichiometric gas mixtures vs. initial pressure.

For comparison with the experiment pressures at the closed end of the vessel (P_3), reflected detonation calculations were also performed. The theoretical reflected detonation pressure vs. initial pressure is plotted in Figure

9. The reflected detonation pressure is approximately 2.5 times larger than the CJ pressure, as expected from basic reflected shock theory. However, the theoretical pressures are still significantly lower than the measured pressures at the reflecting end (P_3). The calculated reflected pressures are approximately 1.8 times lower than the measured values for initial pressures of 150 to 337 psi, and more than 3 times lower for 125 psi initial pressure. These results further suggest that the detonation is in fact unstable and overdriven, and so simple one-dimensional, steady shock and detonation theory cannot capture the complete physics.

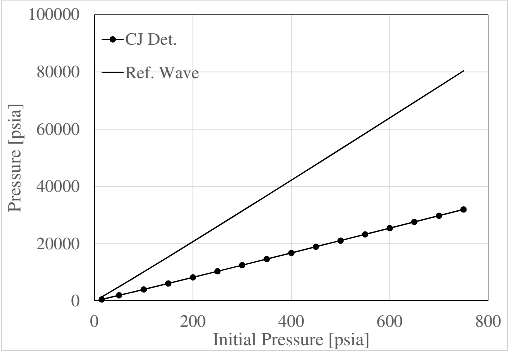

Figure 9: Comparison of theoretical CJ detonation and reflected detonation pressures for stoichiometric ethylene-nitrous oxide vs. initial pressure.

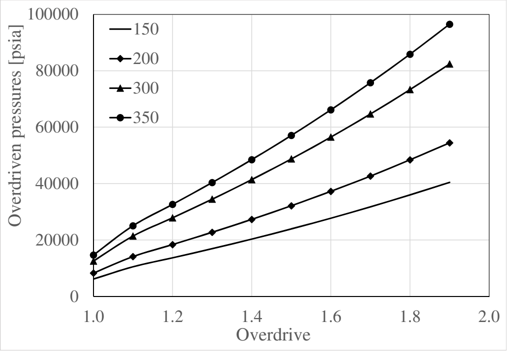

Figure 10: Theoretical overdriven detonation pressures for stoichiometric ethylene-nitrous oxide for initial pressures of 150, 200, 300 and 350 psia.

Finally, calculations of overdriven detonations were performed to investigate if the predicted pressures would more closely match the experimental pressures. The theoretical pressures for stoichiometric ethylene-nitrous oxide were calculated for initial pressures of 150, 200, 300 and 350 psia and overdrive factors of 1 to 1.9. The resulting theoretical overdrive pressures are shown in Figure 10. Comparing the calculated results to the experimental data (with estimated overdrive factors) given in Table 2, we observe that in some cases the overdriven pressure is larger and in some cases smaller than the corresponding measured pressure. For example, for an initial pressure of 200 psi we measured pressures of 15406 psia and 29192 psia for overdrive factors of 1.31 and 1.22, respectively. The theoretical pressures for overdrive factors of 1.3 and 1.2 are 22718 psia and 18363 psia, larger than the corresponding measured pressure for $f = 1.3$ and lower for $f = 1.2$. These oscillations in the measured pressures are attributed to the instability in the reaction of the gas mixture.

The instability associated with multi-step reactions can be explained using studies by Short and Quirk [20] and Short and Sharpe [21] which have shown a direct dependence of detonation instability on the ratio of induction length to energy release zone length, τ/δ. The authors found that the degree of instability increased if this ratio increased. This ratio was calculated for a stoichiometric mixture of ethylene-nitrous oxide, ethylene-oxygen, ethylene-air, hydrogen-oxygen and hydrogen-air using Cantera and plotted in Figure 11. The values for the other mixtures act as comparison. The large values of τ/δ for ethylene nitrous oxide are indicative of strong instabilities in the detonations when compared to the other reactant combinations. This detonation instability manifests as oscillations of the shock front and it propagates along the length of the test tube.

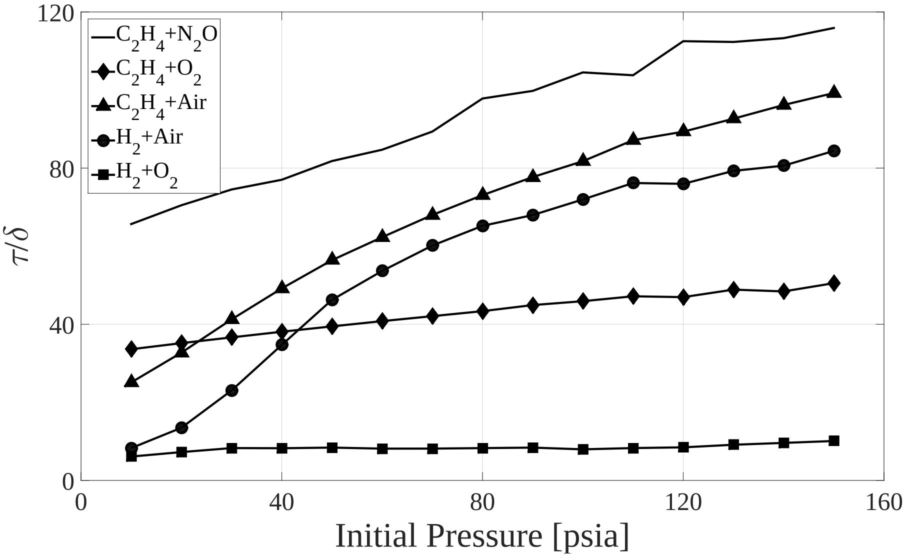

Figure 11: Variation of tau/delta with initial pressure.

4. Testing in a Large L/d Tube

The data from the tests in Section 3 indicates inconsistent pressures between tests of the same initial pressure. As discussed in the previous section, it is believed that an overdriven detonation develops and the small L/d (6.13) of the tube doesnt allow the detonation to decay to a stable state. To observe the steady state detonation, a second vessel with a larger L/d of 68.18 was designed and fabricated. Again, this work investigates the high pressure combustion characteristics of a stoichiometric mixture of ethylene and nitrous oxide ($C_2H_4 + 6N_2O$). The focus of this series of experiments is to investigate the consistency in detonation parameters between tests of same initial pressures for a stoichiometric mixture of ethylene and nitrous oxide. Preliminary testing was conducted at an initial pressure of 50 psia.

4.1. Methods

The R4 reactor vessel used for the first test series was replaced with the test tube shown in Figure 11. The tube was designed and fabricated at Purdue University using a 1.5" XX-Heavy pipe, and was hydrostatically tested to 10,000 psi at Zucrow Laboratories prior to assembly. The test tube has an internal length of 75 in. and an internal diameter of 1.1 in. (L/d = 68). As shown in Figure 12, the tube can accommodate 12 high pressure (100,000 psia) transducers, 6 in. apart, to measure pressure peaks at each location along the length of the tube during the propagation of the combustion wave and one at the end wall to measure the reflected pressure. The transducers are connected to a high frequency data acquisition system via signal conditioning and pressure data is collected at a sampling rate of 600,000 samples/s/channel. The inflow of propellants and venting of the combustion gases is carried out by the same plumbing used on the previous setup.

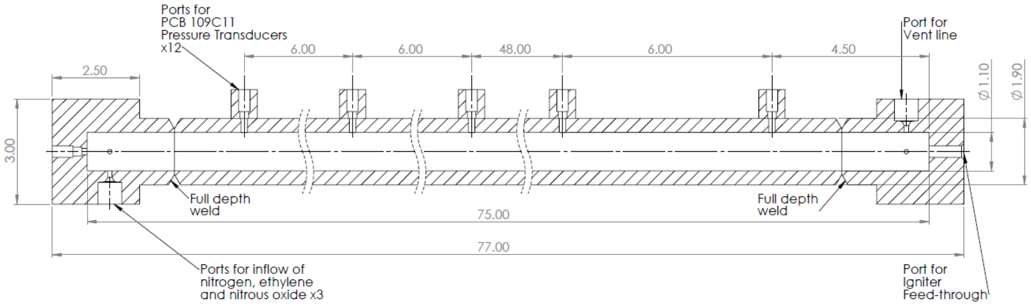

Figure 12: Diagram of the large L/d test tube.

The plumbing for the fuel and oxidizer includes separate sonic venturis that are used to set mass flow rates of the two gases resulting in the appropriate final pressure for each test. The partial pressures of ethylene and nitrous oxide supplied to the vessel are calculated to achieve a stoichiometric fuel-oxidizer mixture. The test tube is heated to approximately 85^{o}F (30^{o}C) using a tape heater to prevent condensation at high pressures.

A Kemlon feed-through was used at the end where the combustion gases are vented, referred to as the vent end. A nichrome bridge wire soldered to the leads of the feed-through functions as an igniter and is energized using an 18 V Li-Po battery when a solid state relay was closed. The ethylene and nitrous oxide gases flow into the vessel from opposing ports to facilitate mixing of the gases. Pressurizing the vessel with ethylene and nitrous oxide is controlled by auto-sequence via a LabVIEW interface, and the gases are further allowed to mix via diffusion for approximately 45 seconds before igniting the mixture. All other procedures followed during testing remained similar to those used during the earlier test series.

4.2. Experimental Results

Preliminary experimental runs were conducted at an initial pressure of 50 psia and four tests were carried out to assess repeatability. The explosion pressures for Test 38 are shown in Figure 13 to illustrate the typical measurements in the tube during a test. The relatively gradual pressure rise recorded by the 1st pressure transducer shows that the combustion wave is still a deflagration at this location. Beyond the 2nd pressure transducer the time interval between pressure peaks measured by consecutive pressure transducers is approximately consistent. This is a good indication that the detonation is propagating at constant velocity as the pressure transducers are equally spaced.

The peak pressures measured from each test run are plotted versus pressure transducer locations and shown in Figure 14. The theoretical CJ detonation pressure, marked using dashes and dots, and reflected detonation pressure, marked using dashes, are calculated using Cantera and are superimposed on the plots for reference. Both the measured detonation and reflected pressures were higher than the theoretical calculations similar to the data from the previous test series. The sudden rise in peak pressure observed between locations 2 and 4 indicate a transition from deflagration to detonation during these tests. Apart from the sudden changes in the peak pressures post-DDT at certain locations, the peak pressures remained approximately constant at some of the mid-range transducer locations. This oscillating behavior can be explained by the detonation instability associated with the reaction of ethylene-nitrous oxide mixtures as discussed in Section

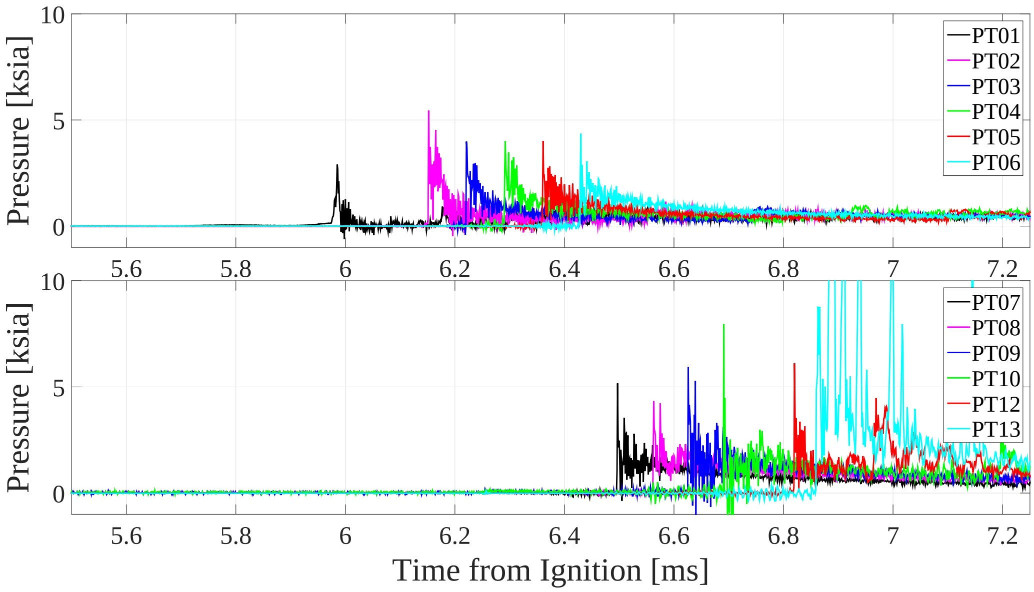

Figure 13: Pressure plots for Test 38 with 50 psia stoichiometric ethylene and nitrous oxide.

3.2. The reflected pressures measured at location 13 shown in Figure 14 are higher than the average pressures measured along the length of the tube, similar to the theoretical comparison presented in Section 3.2. The average pressure in the tube, excluding the pressure at location 13, varies between 4780 and 5150 psia, while the reflected pressures vary between 7575 and 8785 psia.

Based on the time instances of these pressure peaks and using the distance between transducers, the propagation speeds of the combustion waves were estimated and are plotted versus pressure transducer locations in Figure 15. The CJ detonation velocity, calculated using Cantera, is marked using dashes in Figure 15 for reference. It is observed that the flame accelerates rapidly between locations 4 and 5 for Test 23, locations 3 and 4 for Tests 24 and 25, and locations 2 and 3 for Test 38, and undergoes a transition to detonation. This DDT mechanism is explained by Lee [19] and is characterized by the generation of an initial overdriven shock wave which is evident in Figure 15.

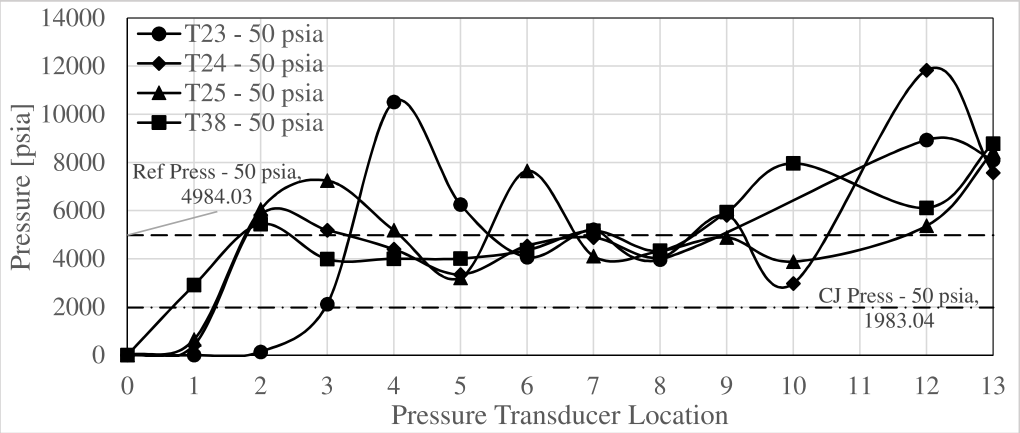

Figure 14: Peak pressures vs. transducer locations for 50 psia stoichiometric ethylene-nitrous tests in the large L/d tube.

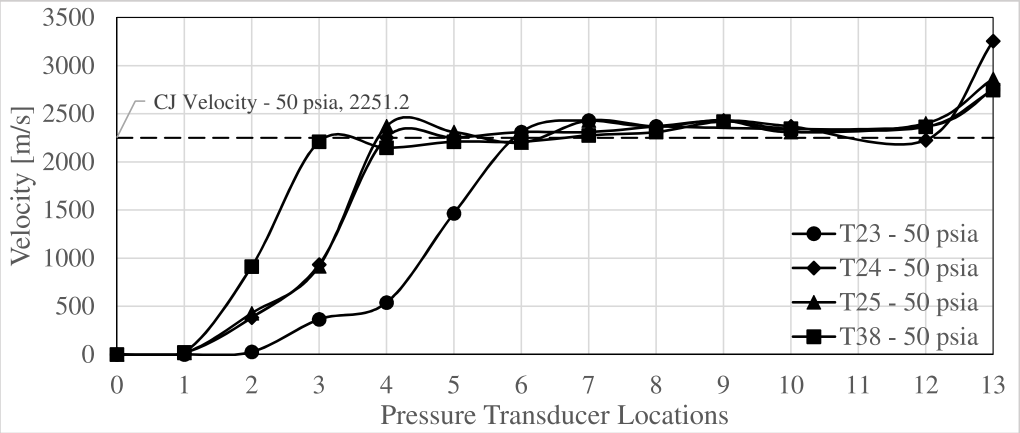

Figure 15: Velocity vs. transducer locations for 50 psia stoichiometric ethylene-nitrous tests in the large L/d tube.

5. Conclusions

In all of the experiments conducted thus far, deflagration-to-detonation (DDT) transition was observed and occurs between the igniter and the first pressure transducer in the smaller L/d tube. This transition occurs at a later location in the larger L/d tube, but tests were conducted at an initial pressure at least 3 times lower than those tests in the reactor vessel. In all cases, the measured pressures significantly exceeded the theoretical CJ detonation pressures. Given that the ignition energy is far too low to achieve direct initiation, the mechanism of DDT is believed to be rapid acceleration and self-turbulizing of the flame front coupled with compression by reflected pressure waves, leading to localized explosions. These explosions generate shock waves that eventually couple with a reaction zone to form a detonation. This theory explains the very high pressures measured by the pressure transducers, as the shock wave will be highly overdriven compared to a CJ detonation, and therefore the pressures would be significantly larger. From estimates of the wave speed, in at least part of the reactor and the large L/d tube, the velocity exceeded the CJ velocity, indicating an overdriven detonation. The rapid and violent DDT observed is caused by a combination of detonation instability of the micture, the high initial pressures, and the degree of confinement inside the reactor.

The results of the experiments in the reactor suggest that obtaining a stable detonation near the CJ state is not possible due its small L/d ratio. The overdriven detonation wave does not have sufficient propagation distance to decay to a stable state, and therefore the reflected pressure measured at the end of the tube is much larger than the predicted reflected pressure. Therefore, a test tube with a larger L/d was designed and preliminary experiments conducted in this tube indicate that the overdriven detonation wave does in fact decay to a velocity close to the CJ detonation velocity. Further experiments will be conducted in the large L/d tube at different initial pressures to assess the effect on the stability and DDT of this mixture. Ion probes will also be added to the existing instrumentation on the large L/d tube; these measurements will allow us to more accurately estimate the wave speed and to identify where DDT occurs. A theoretical study and computational modeling of the detonation characteristics will also be conducted simultaneous to the ongoing experimental work.

6. Acknowledgements

This work is supported by Sandia National Laboratories. Sandia National Laboratories is a multi-program laboratory managed and operated by Sandia Corporation, a wholly owned subsidiary of Lockheed Martin Corporation, for the U.S. Department of Energy's National Nuclear Security Administration under contract DE-AC04-94AL85000. The support and expertise of the Maurice Zucrow Laboratory staff and students has been invaluable in the progress of this work.

7. References

[1] R. W. Humble, G. N. Henry, W. J. Larson, Space propulsion analysis and design, McGraw-Hill, 1995.

[2] M. J. Tauschek, L. C. Corrington, M. C. Huppert, Nitrous oxide supercharging of an aircraft engine cylinder, Naca wartime report e-199, National Advisory Committee for Aeronautics. Lewis Flight Propulsion Lab, Cleveland, OH, United States (jun 1945).

[3] J. Laughrey, L. Bollinger, R. Edse, Detonability of nitrous oxide at elevated initial temperature and pressure, Tech. rep. (1962).

[4] A. Jost, K. Michel, J. Troe, H. G. Wagner, Detonation and shock-tube studies of hydrazine and nitrous oxide, Tech. rep. (1963).

[5] L. Bollinger, J. Laughrey, R. Edse, Experimental detonation velocities and induction distances in hydrogen-nitrous oxide mixtures, ARS Journal (32) (January 1962) 81–82.

[6] G. Johnson, W. Barton, J. Brothers, S. Bryan, P. Gauglitz, R. Hill, L. Pederson, C. Stewart, L. Stock, Evaluation of High-Level Nuclear Waste Tanks Having a Potential Flammable Gas Hazard, Pacific Northwest National Laboratory, 1997.

[7] M. Kaneshige, R. Akbar, J. Shepherd, Hydrocarbon-air-nitrous oxide detonations, Spring Meeting of the Western States Section of the Combustion Institute.

[8] M. Kaneshige, E. Schultz, U. Pfahl, J. Shepherd, R. Akbar, Detonations in mixtures containing nitrous oxide, in: Proceedings of the 22nd international symposium on shock waves, Imperial College, London, UK, Vol. 1, 2000, pp. 251–256.

[9] R. Mével, F. Lafosse, N. Chaumeix, G. Dupré, C.-E. Paillard, Spherical expanding flames in h 2–n 2 o–ar mixtures: flame speed measurements and kinetic modeling, international journal of hydrogen energy 34 (21) (2009) 9007–9018.

[10] S. Bane, R. Mével, S. Coronel, J. Shepherd, Flame burning speeds and combustion characteristics of undiluted and nitrogen-diluted hydrogen–nitrous oxide mixtures, international journal of hydrogen energy 36 (16) (2011) 10107–10116.

[11] C. Merrill, Nitrous oxide explosive hazards, Tech. rep. (2008).

[12] M. Grubelich, J. Rowland, L. Reese, A hybrid rocket engine design for simple low cost sounding rocket use, in: Joint Propulsion Conference and Exhibit, Vol. 1, 1993.

[13] J. S. Tyll, R. Herdy, The nitrous oxide-propane rocket engine gasl tr no. 387, Tech. rep., MICRO CRAFT INC HUNTSVILLE AL (2001).

[14] R. DiSalvo, M. Ostrander, A. Elliott, Constant volume rocket motor, uS Patent 7,631,487 (2009).

[15] J. Foust, The space review: Essays and commentary about the final frontier.

[16] J. Joannon, Detonability limits of gaseous mixtures in cylindrical smooth tubes (1991).

[17] S. Browne, J. Shepherd, J. Ziegler, Shock and detonation toolbox, 2005. URL `www2.galcit.caltech.edu/EDL/public/cantera/html/SD_Toolbox/index.html`

[18] D. Goodwin, Cantera: Object-oriented software for reacting flows, Technical report, California Institute for Technology (Caltech), www.code.google.com/p/cantera.

[19] J. H. Lee, The detonation phenomenon, Vol. 2, Cambridge University Press Cambridge, 2008.

[20] M. Short, J. J. Quirk, On the nonlinear stability and detonability limit of a detonation wave for a model three-step chain-branching reaction, Journal of Fluid Mechanics 339 (1997) 89–119.

[21] M. Short, G. J. Sharpe, Pulsating instability of detonations with a two-step chain-branching reaction model: theory and numerics, Combustion Theory and Modelling 7 (2) (2003) 401–416.